Iranian Journal of Numerical Analysis and Optimization
Vol. 15, No. 1, 2025, pp 346–374
https://doi.org/10.22067/ijnao.2024.88564.1461
https://ijnao.um.ac.ir/

Research Article

Dynamical analysis of a nonlinear oscillator chain in the Peyrard–Bishop DNA model using residual power series and Laplace residual power series method

D. Priyadarsini, P.K. Sahu and M. Routaray*

Abstract

In this study, we investigate the numerical exploration of the Peyrard–Bishop DNA (PBD) dynamic model. These solutions are responsible for analyzing the nonlinear interactions between the adjacent displacements of the DNA strand. To obtain these solutions, the authors present two highly

*Corresponding author

Received 20 June 2024; revised 26 September 2024; accepted 12 October 2024

Dibyajyoti Priyadarsini
Department of Mathematics, School of Applied Sciences, KIIT University, Odisha-751024, India. e-mail:pdibyajyoti7@gmail.com

Prakash Kumar Sahu
Department of Mathematics, Model Degree College, Nayagarh Odisha-752079, India e-mail:prakash.2901@gmail.com

Mitali Routaray
Department of Mathematics, School of Applied Sciences, KIIT University, Odisha-751024, India. e-mail:mitaray8@gmail.com

How to cite this article
Priyadarsini, D., Sahu, P.K. and Routaray, M., Dynamical analysis of a nonlinear oscillator chain in the Peyrard–Bishop DNA model using residual power series and Laplace residual power series method. *Iran. J. Numer. Anal. Optim.*, 2025; 15(1): 346-374. https://doi.org/10.22067/ijnao.2024.88564.1461

effective and precise techniques for solving the nonlinear PBD dynamic model: the Residual Power Series Method (RPSM) and the Laplace Residual Power Series Method (LRPSM), applied under initial and boundary conditions. The concept is explained through various numerical examples, demonstrating its practical application and ease of use. A convergence analysis has been provided between the exact and approximate solutions. These physical characteristics are thoroughly analyzed through graphical representations. The proposed methods are compared with other numerical techniques to showcase their applicability, accuracy, and efficiency. Two test case problems are solved, and the results are presented as tables and figures using MATHEMATICA software. The solutions illustrate the successful applications of the proposed methods, which can assist in finding numerical solutions to other nonlinear problems.

AMS subject classifications (2020): 35R11; 65M25; 65M30.

Keywords: DNA model; Laplace Transform; Power series method; Convergence analysis.

1 Introduction

Nonlinear partial differential equations (NLPDEs) have significance in science and engineering due to their wide range of applications. Most of the real-world situations can be transformed into nonlinear mathematical models. Consequently, solving such a system is significant and requires much investigation. Researchers have been motivated to develop and investigate effective techniques to solve such dynamical systems, which exhibit nonlinearities [11, 26, 9]. A significant part of mathematical modeling involves both linear partial differential equations (LPDEs) and NLPDEs. NLPDEs are particularly useful in addressing problems in quantum mechanics, plasma physics, and nonlinear optics. Two-dimensional random NLPDEs are crucial in numerous applications within engineering, biology, and physics. Many scientific problems are modeled using nonlinear random PDEs with two variables [29, 28, 18, 24].

Over the last few decades, researchers have proposed numerous analytical methods and approximate algorithms for solving NLPDEs. Chakrabarty

et al.[10] explored optical soliton solutions of the complex Ginzburg–Landau (CGL) model with Kerr law nonlinearity. Similarly, Hosseini et al.[19] examined soliton solutions within the same context. Chen et al. [12] investigated the Ivancevic option pricing model, and using the trial function method, they derived rogue wave and dark wave solutions. More recently, Osman [25] obtained multi-soliton rational solutions for the quantum Zakharov–Kuznetsov equation in quantum magnetoplasmas using the generalized unified method. Some other analytical methods have been investigated by several authors[22, 31, 21]. Identifying various approaches is essential for better understanding natural occurrences. This natural occurrence can occur across multiple fields including science, engineering, biology, chemistry, and physics. As the application of NLPDEs develops, researchers begin to develop new methods to solve these differential equations numerically because solving these equations analytically presents numerous challenges. Numerous methods, such as the Adomian decomposition method [7], homotopy perturbation method [30], differential transform method [8], and others, are accessible in the literature.

Recently, scientists have been describing real-world issues with innovative numerical techniques. These days, studying the nonlinear dynamics of deoxyribonucleic acid (DNA) has become a major area of study due to its significance for gene replication, the development of viruses and vaccines, and the underlying mechanisms that govern the transfer of genetic information between generations. In fact, DNA is a biomolecule that contains genetic materials necessary for an organism's growth and reproduction. It consists of two nucleotide linear polymer strands. Sugars, pyrimidine and purine bases, and phosphate make up each strand. Its intricate structure restricts research and makes mathematical modeling challenging.

In this study, we intend to solve a well-known biological model called the Peyrard–Bishop DNA (PBD) model. Peyrard–Bishop was the first to explain this phenomenon, which involved a nonlinear interaction of adjoining shifts and hydrogen bonds. Peyrard and Bishop [27] and Abazari, Jamshidzadeh, and Wang [1] have investigated the oscillator chain of the PBD model to investigate the emergence of solitonic structures. The study of Dusuel, Michaux, and Remoissenet [14] and Alvarez et al. [5] examines

the connections between powerless nonlinearity and scattering in the DNA energetic show, including straight scattering and nonlinear scattering. According to research on the scientific and physical modeling of DNA elements, these criteria can be boiled down to a critical nonlinear configuration. Moreover, hyperbolic and exponential function techniques were employed by Ali et al. [3] to obtain the precise results of this model. Additionally, they looked at a few numerical solutions for the PBD model using the finite difference (FD) approach. Zdravković and Satarić [33] investigated the Peyrard–Bishop–Dauxois model, which is an extended variant of the PBD concept of DNA dynamics. Agüero, De Lourdes Najera, and Carrillo [2] investigated the Hamiltonian PBD model's harmonic potential. As per the literature survey, the PBD model, created to explore DNA dynamics, offers both strengths and weaknesses. Strengths: It effectively captures nonlinear dynamics, particularly the interactions between DNA base pairs, which are essential for understanding denaturation and biological activity. The model's simplicity makes it accessible for both numerical and analytical studies, despite representing complex phenomena. It also provides a useful framework for simulating the thermal separation of DNA strands, aligning well with experimental data. Weaknesses: The model oversimplifies DNA as a one-dimensional chain, neglecting the full three-dimensional helical structure and sequence specificity, which limits its biological accuracy. Although helpful for thermal denaturation studies, the PBD model may not be sufficient for explaining complex molecular processes like DNA-protein interactions or replication, reflecting its limited applicability.

According to the literature study, the PBD model has been solved analytically using various methods. Only one or two scholars have solved this model numerically. So the primary motivation for our research is to find numerical solutions to the PBD model using two different techniques known as the residual power series method (RPSM) and the Laplace residual power series method (LRPSM) which is based on Taylor's series expansion. Both of these methods use symbolic computing software to develop a power series solution as a rapidly convergent series with the least possible computations. The results are very encouraging and the proposed technique is both computationally feasible and reliable.

A useful analytical technique for figuring out the coefficients of the power series solutions of a particular class of differential equations is the RPSM, which was introduced by [17]. Its foundation is the formulation of linearity- and perturbation-free power series solutions to several linear and nonlinear equations. The LRPSM is yet another novel analytical technique that is employed in this work. The technique in the discussion was initially introduced by Eriqat and colleagues [4]. The suggested technique achieves its main goal by utilizing the concept of the limit at infinity, even though it does not depend on the derivative for computing the coefficients of the series solution, as the RPSM approach requires. These two techniques have recently been adapted to solve various types of differential equations, such as nonlinear time-fractional dispersive PDEs [4], hyperbolic systems of Caputo-time-fractional PDEs with variable coefficients [16], time-fractional Navier-Stokes equations [32], space-time fractional PDEs and nonlinear PDE, respectively, [6, 20].

The paper is organized as follows: The importance of the PBD model and its application to a certain field of research are highlighted in section "Introduction". It also mentions the study's main objectives, as well as any background information necessary for understanding the next sections. The following section discusses the way the PBD model is formed. The section titled "Numerical methods for the PBD model equation" describes the proposed numerical technique for determining solutions for the PBD Model equation. The next section examines the "Convergence analysis," which estimates how closely the numerical solution approximates the exact solution. In Section "Illustrative examples," the proposed method is used to solve the nonlinear PBD Model equation problem of accuracy and applicability. The work's contributions are summarized in the "Conclusion" section, which emphasizes the suggested method's achievements and provides potential directions for further research.

2 Formation of PBD model

A DNA molecule is generally shaped like a double helix, which means it is made up of two complimentary polymeric chains that are wrapped around one

another. In the Watson–Crick model [23], B-shaped DNA generates a double helix containing a pair of strands. The masses of nucleotides vary by minimal amounts, indicating a homogeneous crystal structure. Hydrogen bonds join the strands, making them weak, however, the harmonic longitudinal length stays strong. In 1989, Peyrard and Bishop proposed the Hamiltonian model [27], which is based on Morse's potential:

$$P_m(w_n - v_n) = \mathcal{D}_e \left\{ e^{-\rho(w_n - v_n)} - 1 \right\}^2. \tag{1}$$

Here, P_m symbolizes Morse's potential, w_n represents the displacement between two atoms, and v_n indicates bond length equilibrium. The parameters $\mathcal{D}_e$ and ρ represent the depth and width of the Morse potential, respectively. Zdravković and Satarić [33] proposed an explanation for the Hamiltonian of the DNA chain. In addition, Dauxois [13] developed an enhanced version of the PB model, which was used in the hydrogen bond strand width defined by the Hamiltonian shown below:

$$\mathcal{H}(w) = \frac{1}{2m}\mathrm{q}^{n^2} + \frac{l_1}{2}\Delta^2 w_n + \frac{l_2}{4}\Delta^4 w_n + \delta(e^{-\rho\sqrt{2}w_n})^2, \tag{2}$$

$$\Delta w_n = w_{n+1} - w_n.$$

In the expression, l_1 and l_2 indicate the linear and nonlinear coupling strengths, respectively. The constant δ is included, and $q_n = mw^n$ represents the momentum of the displacement w_n. Starting with the Hamiltonian equation (2), the equation of motion in the continuum limit can be stated as follows.

$$w_{\tau\tau} - (k_1 + 3k_2 w_{ss}) - 2\sqrt{2}\rho D_e e^{-\alpha w}(e^{-\alpha w} - 1) = 0. \tag{3}$$

Define parameters as follows: $k_1 = \frac{l_1}{m}d_1^2$, $k_2 = \frac{l_2}{m}d_1^4$, $D_e = \frac{\delta}{m}$, and $\alpha = \sqrt{2}\rho$, where d_1 represents the inter-site nucleotide length in the DNA ladder.

This paper examines the PBD model equation as follows:

$$w_{\tau\tau} - (k_1 + 3k_2 w_s^2)w_{ss} - 2\alpha\varpi e^{-\alpha w}(e^{-\alpha w} - 1) = 0 \tag{4}$$

with initial condition

$$w(s,0) = \frac{-1}{\alpha}\ln\left(\pm\frac{2\sqrt{3}\sqrt{k_2}}{\alpha^2\sqrt{\Omega}}\mathrm{sech}^2 s\right), \tag{5}$$

where k_1, k_2, α, β, and $\varpi = D_e$ are real parameters. We will then go over the fundamentals of using the RPSM and LRPSM methods to solve the nonlinear PBD model equation.

3 Basic concepts

Definition 1. [17] An expansion of the form

$$\sum_{n=0}^{\infty} \phi_n(s)(\tau-\tau_0)^n = \phi_0(s) + \phi_1(s)(\tau-\tau_0) + \phi_2(s)(\tau-\tau_0)^2 + \cdots, \quad 0 \le n-1 \le n,\ \tau \ge \tau_0, \tag{6}$$

is referred to as a power series around $\tau = \tau_0$, in which τ is the variable and $\phi_n(s)$ is the coefficient of the series and function of s.

Theorem 1. [17] Let $w(s,\tau)$ have the following power series representation of $\tau_0 = 0$

$$w(s,\tau) = \sum_{n=0}^{\infty} \phi_n(s)\tau^n, \qquad s \in I, 0 \le \tau < R. \tag{7}$$

The coefficients $\phi_n(s)$ of the equation can be defined as follows:

$$\phi_n(s) = \frac{\partial_\tau^n w(s,0)}{n!},$$

For $n = 0, 1, 2\ldots$, $\partial_\tau^n = \frac{\partial^n}{\partial \tau^n}$, and $R = \min_{c \in I} R_c$, where R_c is the radius of convergence of the power series $\sum_{n=0}^{\infty} \phi_n(s)\tau^n$. Now, substituting $\phi_n(s)$ into the series representation (7) yields an expansion, which is an expansion of variable coefficients,

$$w(s,\tau) = \frac{\partial_\tau^n w(s,0)}{n!}\tau^n, \qquad x \in I, 0 \le \tau < R. \tag{8}$$

Definition 2. Let $w(s,\tau)$ be a function defined for $\tau > 0$. The Laplace transform of $w(s,\tau)$, providing the integral converges on an integral of s, is defined as

$$W(s,p) = \mathfrak{L}\big[w(s,\tau)\big] = \int_0^{\infty} e^{-p\tau} w(s,\tau) d\tau. \tag{9}$$

Definition 3. The inverse Laplace transform of a function $W(s,p)$ is the function $w(s,\tau), \tau \ge 0$, defined as

$$w(s,\tau)=\mathfrak{L}^{-1}[W(s,p)]=\int_{r-i\infty}^{r+i\infty}e^{p\tau}W(s,p)dp,\qquad r=Re(p)>a_0,\quad(10)$$

where a_0 lies in the right half plane of the integral's absolute convergence.

Lemma 1. [15] Let $\partial_\tau^{m-1}w_1(s,\tau)$, $\partial_\tau^{m}w_1(s,\tau)$, $\partial_\tau^{m-1}w_2(s,\tau)$, and $\partial_\tau^{m}w_2(s,\tau)$ be piece-wise continuous functions of exponential order ϵ defined on $I\times[0,\infty)$, $m=1,2,\ldots,n$. Assume $\mathfrak{L}[w(s,\tau)]=W(s,p)$, $\mathfrak{L}^{-1}[W(s,p)]=w(s,\tau)$ in which $(s,p)\in F=\{(s,p):\sqrt{s^2+p^2}>\epsilon(s)\}$, where α and β are constants. Then the remaining conditions are satisfied

1. $\mathfrak{L}[\alpha w_1(s,\tau)+\beta w_2(s,\tau)]=\alpha W_1(s,p)+\beta W_2(s,p),\ s\in I,\ p>\epsilon,$
2. $\mathfrak{L}^{-1}[\alpha W_1(s,p)+\beta W_2(s,p)]=\alpha w_1(s,\tau)+\beta w_2(s,\tau),\ s\in I,\ \tau\geq 0,$
3. $\mathfrak{L}[\partial_\tau w(s,\tau)]=p\mathfrak{L}[w(s,\tau)]-w(s,0),$
4. $\mathfrak{L}[\partial_\tau^2 w(s,\tau)]=p^2\mathfrak{L}[w(s,\tau)]-w_\tau(s,0)-pw(s,0),$
5. $\mathfrak{L}[\partial_\tau^n w(s,\tau)]=p^n\mathfrak{L}[w(s,\tau)]-\sum_{m=0}^{n-1}p^{n-m-1}\partial_\tau^m w(s,0),$
6. $\lim_{p\to\infty}W(s,p)=0,$
7. $\lim_{p\to\infty}pW(s,p)=w(s,0).$

Theorem 2. Let the function $W(s,p)=\mathfrak{L}[w(s,\tau)]$ can be expressed as Laurent series representation:

$$W(s,p)=\frac{\phi_0(s)}{p}+\sum_{n=1}^{\infty}\frac{\phi_n(s)}{p^{n+1}},\qquad s>0,\ s\in I.\qquad(11)$$

Then, $\phi_n(s)=\frac{\partial^n}{\partial\tau^n}w(s,0),\ n=0,1,2,\ldots.$

Proof. Assume that $W(s,p)$ is represented by the Laurent series expansion of (11). Subsequently, we have

$$pW(s,p)=\phi_0(s)+\sum_{n=1}^{\infty}\frac{\phi_n(s)}{p^n},\qquad p>0.\qquad(12)$$

Also, $\phi_0(s)=w(s,0)$.

Now, multiplying p on (12), we obtain

$$\begin{aligned} p^2W(s,p) - pw(s,0) &= \phi_1(s) + \sum_{n=2}^{\infty} \frac{\phi_n(s)}{p^n}, \\ \phi_1(s) &= p^2W(s,p) - pw(s,0) - \sum_{n=2}^{\infty} \frac{\phi_n(s)}{p^n}. \end{aligned} \tag{13}$$

Now, our aim is to find the value of $\phi_1(s)$. Therefore, we arrange (13) as $p \to \infty$ on both sides

$$\begin{aligned} \phi_1(s) &= \lim_{p\to\infty} (p^2W(s,p) - pw(s,0) - \sum_{n=2}^{\infty} \frac{\phi_n(s)}{p^n}) \\ &= \lim_{p\to\infty} (p^2W(s,p) - pw(s,0)) \\ &= \lim_{p\to\infty} p(pW(s,p) - w(s,0)) \\ &= \lim_{p\to\infty} p(\mathfrak{L}\,[w_\tau(s,\tau)]) \\ &= w_\tau(s,0). \end{aligned}$$

To derive the general formula for $\phi_n(s)$, multiply (12) by p^{n+1} and take the limit of the generated equation as $p \to \infty$. This gives $\phi_n(s) = \frac{\partial^n}{\partial \tau^n} w(s,0), \quad n = 0, 1, 2, \ldots$. □

Next, we shall investigate the numerical solution for the PBD dynamic model equation using the numerical methods.

4 Numerical methods

In this section, we give a detailed view of the RPSM and LRPSM used to find the solution of the model in (4).

4.1 Residual power series method (RPSM)

In this section, we apply the RPSM to solve the PBD dynamic model equation given as

$$w_{\tau\tau} - (k_1 + 3k_2w_s^2)w_{ss} - 2\alpha\varpi e^{-\alpha w}(e^{-\alpha w} - 1) = 0.$$

The initial condition for (4) has been defined as

$$w(s,0) = \frac{-1}{\alpha} \ln \left(\pm \frac{2\sqrt{3}\sqrt{k_2}}{\alpha^2 \sqrt{\Omega}} \operatorname{sech}^2 s \right). \tag{14}$$

We utilize RPSM to obtain a series solution to the given equation under the specified initial conditions. This entails replacing the power series expansion with the reduced residual function. The resulting equation provides a recurrence formula for the truncated residual function.

Assume that the solution is in the expansion form:

$$w(s,\tau) = \sum_{n=0}^{\infty} \phi_n(s)\tau^n, \qquad 0 \le \tau < \mathbb{R}, s \in \mathbb{I}. \tag{15}$$

Next, kth truncated series of w be defined in the form of w_k:

$$w_k(s,\tau) = \sum_{n=0}^{k} \phi_n(s)\tau^n, \qquad 0 \le \tau < \mathbb{R}, s \in \mathbb{I}. \tag{16}$$

For $w(s,0) = \phi_0(s) = \phi(s)$, (14) can be written as

$$w_k = \phi(s) + \sum_{n=1}^{k} \phi_n(s)\tau^n, \qquad 0 \le \tau < \mathbb{R}, s \in I, k = 1, \infty. \tag{17}$$

In order to determine the coefficients $\phi_n(s)$ for $n = 1, 2, 3, \ldots, k$ in the series expansion of (17), the residual function is defined as follows:

$$Res_w = w_{\tau\tau} - (k_1 + 3k_2 w_s^2) w_{ss} - 2\alpha\varpi e^{-\alpha w}(e^{-\alpha w} - 1). \tag{18}$$

Then, the kth residual function, Res_k, where $k = 1, 2, \ldots$ is as follows:

$$Res_w^k = (w_k)_{tt} - (k_1 + 3k_2 (w_k)_s^2)(w_k)_{sss} - 2\alpha\varpi e^{-\alpha(w_k)}(e^{-\alpha(w_k)} - 1). \tag{19}$$

According to literature, $Res_w = 0$ and $\lim_{k\to\infty} Res_w^k = Res_w$ for all $s \in I$ and $\tau \ge 0$. Then, $(\partial^{r-1} Res_w / \partial\tau^{r-1}) = 0$. for every $r = 1, 2, \ldots, k$. Now, calculate $\phi_1(s)$, using (19) as

$$Res_w^1 = (w_1)_{tt} - (k_1 + 3k_2 (w_1)_s^2)(w_1)_{ss} - 2\alpha\varpi e^{-\alpha(w_1)}(e^{-\alpha(w_1)} - 1), \tag{20}$$

where

$$w_1 = \phi(s) + t\phi_1(s)$$

and

$$\phi(s) = w(s,0) = \frac{-1}{\alpha} ln \left(\pm \frac{2\sqrt{3}\sqrt{k_2}}{\alpha^2\sqrt{\Omega}} \text{sech}^2 s \right).$$

We derive that $Res_1 = 0$ $(\tau = 0)$ from (20), and consequently,

$$\phi_1(s) = 0.332348 \tanh(s).$$

The first RPS approximate solution is

$$w_1 = -\log(1.09545 \text{ sech}(s)) + \tau 0.332348 \tanh(s).$$

To determine the form of $\phi_2(s)$, the second unknown coefficient,

$$w_2 = \phi(s) + \tau\phi_1(s) + \tau^2\phi_2(s).$$

Using $k = 2$ in (19), the residual function becomes

$$Res_w^2 = (w_2)_{tt} - (k_1 + 3k_2(w_2)_s^2)(w_2)_{ss} - 2\alpha\varpi e^{-\alpha(w_2)}(e^{-\alpha(w_2)} - 1). \quad (21)$$

Moreover, $(\partial Res_w^2/\partial\tau) = 0$ in $Res_w^2(\tau = 0)$, and consequently,

$$\phi_2(s) = 0.213317 \text{ sech}(x)^{\frac{1}{\sqrt{2}}} - 0.22752 \text{ sech}(x)^{\sqrt{2}}.$$

Thus, the second RPS approximate solution is

$$\begin{aligned} w_2(s,\tau) = &-\log(1.09545 \text{ sech}(s) + t0.332348 \tanh(s) \\ &+ \tau^2(0.213317\text{sech}(s)^{\frac{1}{\sqrt{2}}} - 0.22752 \text{ sech}(s)^{\sqrt{2}}). \end{aligned}$$

Similarly, we write the next approximation as

$$w_3 = \phi(s) + \tau\phi_1(s) + \tau^2\phi_2(s) + \tau^3\phi_3(s).$$

For $k = 3$ in (19),

$$Res_w^3 = (w_3)_{\tau\tau} - (k_1 + 3k_2(w_3)_s^2)(w_3)_{ss} - 2\alpha\varpi e^{-\alpha(w_3)}(e^{-\alpha(w_3)} - 1), \quad (22)$$

$(\partial^2 Res_w^3/\partial\tau^2) = 0(\tau = 0)$, and thus

$$\phi_3(s) = 0.0534688 \text{ sech}(s)^{1+\sqrt{2}} \sinh(s).$$

Therefore, the third approximate solution becomes

$$\begin{aligned} w_3(s,\tau) = &- \log(1.09545\ \mathrm{sech}(s) + t0.332348\tanh(s) \\ &+ \tau^2(0.213317\mathrm{sech}(s)^{\frac{1}{\sqrt{2}}} - 0.22752\ \mathrm{sech}(s)^{\sqrt{2}}) \\ &+ \tau^3 0.0534688\ \mathrm{sech}(s)^{1+\sqrt{2}}\sinh(s). \end{aligned}$$

We repeat this procedure to represent the solution to (4). The kth-approximation of the solution to (4) can be stated in the following finite series:

$$\begin{aligned} &w_k(s,\tau) \\ &= -\log(1.09545\ \mathrm{sech}(s) + t0.332348\tanh(s) + t^2(0.213317\ \mathrm{sech}(s)^{\frac{1}{\sqrt{2}}} \\ &\quad - 0.22752\ \mathrm{sech}(s)^{\sqrt{2}}) + \tau^3 0.0534688\ \mathrm{sech}(s)^{1+\sqrt{2}}\sinh(s) + \cdots. \end{aligned}$$

4.2 Laplace residual power series method (LRPSM)

In this section, we explain the steps of the LRPSM used to solve the PBD model (4). The LRPSM's primary technique involves applying the Laplace transform to NLPDEs and using a power series as the proposed solution within this transformed space. The coefficients of this expansion, which represent unknowns, are found using a technique similar to the standard RPSM. Ultimately, the solution obtained in the transformed space is reverted to the original space using the inverse Laplace transform, thus providing the solution for the PBD model equation.

step 1: First, we apply the Laplace transform to (4), that is,

$$\begin{aligned} \mathfrak{L}[w_{\tau\tau}] &= \mathfrak{L}\big[(k_1 + 3k_2 w_s^2)w_{ss}\big] + \mathfrak{L}\big[2\alpha\varpi e^{-\alpha w}(e^{-\alpha w} - 1)\big] \\ &= \mathfrak{L}\big[(k_1 + 3k_2 w_s^2)w_{ss}\big] + 2\alpha\varpi\mathfrak{L}\left[e^{-2\alpha w}\right] - 2\alpha\omega\mathfrak{L}\left[e^{-\alpha w}\right] \\ &= \mathfrak{L}\big[(k_1 + 3k_2 u_s^2)w_{ss}\big] + 2\alpha\varpi\mathfrak{L}\left[\sum_{n=0}^{\infty}\frac{(-1)^n 4^n \alpha^n}{n!}w^n(s,\tau))\right] \\ &\quad - 2\alpha\varpi\mathfrak{L}\left[\sum_{n=0}^{\infty}\frac{(-1)^n \alpha^n}{n!}w^n(s,\tau))\right]. \end{aligned} \tag{23}$$

Using $\mathfrak{L}[w_{\tau\tau}(s,\tau)] = p^2\mathfrak{L}[w(s,\tau)] - w_\tau(s,0) - pw(s,0)$ with initial condition given in (14), we write (23) as

$$
\begin{aligned}
&p^2\mathfrak{L}[w(s,\tau)] - w_\tau(s,0) - pw(s,0)\\
&\quad = k_1 W_{ss}(s,p) + 3k_2\mathfrak{L}\left[\mathfrak{L}^{-1}[W_s(s,p)]^2\mathfrak{L}^{-1}[W_{ss}(s,p)]\right]\\
&\qquad + 2\alpha\varpi\sum_{n=0}^{\infty}\frac{(-1)^n}{n!}4^n\alpha^n\mathfrak{L}\left[\mathfrak{L}^{-1}\left[W(s,p)\right]^n\right]\\
&\qquad - 2\alpha\varpi\sum_{n=0}^{\infty}\frac{(-1)^n\alpha^n}{n!}\mathfrak{L}\left[\mathfrak{L}^{-1}\left[W(s,p)\right]^n\right],
\end{aligned}
$$

$$
\begin{aligned}
&W(s,p)\\
&= \frac{\phi_0(s)}{p} + \frac{\phi_1(s)}{p^2} + \frac{k_1 W_{ss}(s,p)}{p^2} + \frac{3k_2}{p^2}\mathfrak{L}\left[\mathfrak{L}^{-1}[W_s(s,p)]^2\mathfrak{L}^{-1}[W_{ss}(s,p)]\right]\\
&\quad + \frac{2\alpha\varpi}{p^2}\sum_{n=0}^{\infty}\frac{(-1)^n 4^n\alpha^n}{n!}\mathfrak{L}\left[\mathfrak{L}^{-1}\left[W(s,p)\right]^n\right]\\
&\quad - \frac{2\alpha\varpi}{p^2}\sum_{n=0}^{\infty}\frac{(-1)^n}{n!}\alpha^n\mathfrak{L}\left[\mathfrak{L}^{-1}\left[W(s,p)\right]^n\right],
\end{aligned}
\tag{24}
$$

where $W(s,p) = \mathfrak{L}[w(s,\tau)]$, $w(s,0) = \phi_0(s)$ and $w_\tau(s,0) = \phi_1(s)$.

step 2: Now, the transformed function $W(s,p)$ can be expressed as the following expansion:

$$
W(s,p) = \sum_{n=0}^{\infty}\frac{\phi_n(s)}{p^{n+1}}. \tag{25}
$$

The kth truncated series is expressed as

$$
W_k(s,p) = \sum_{n=0}^{k}\frac{\phi_n(s)}{p^{n+1}} = \frac{\phi_0(s)}{p} + \sum_{n=1}^{k}\frac{\phi_n(s)}{p^{n+1}}.
$$

Now, by using the Laplace residual function to (24), it is as follows:

$$
\begin{aligned}
LRes_W(s,p) =& W(s,p) - \frac{\phi_0(s)}{p} - \frac{\phi_1(s)}{p^2} - \frac{k_1}{p^2}W_{ss}(s,p)\\
&- \frac{3k_2}{p^2}\mathfrak{L}\left[\mathfrak{L}^{-1}[W_s(s,p)]^2\mathfrak{L}^{-1}[W_{ss}(s,p)]\right]\frac{2\alpha\varpi}{p^2}\\
&- \sum_{n=0}^{\infty}\frac{(-1)^n}{n!}4^n\alpha^n\mathfrak{L}\left[\mathfrak{L}^{-1}\left[W(s,p)\right]^n\right]\\
&+ \frac{2\alpha\varpi}{p^2}\sum_{n=0}^{\infty}\frac{(-1)^n\alpha^n}{n!}\mathfrak{L}\left[\mathfrak{L}^{-1}\left[W(s,p)\right]^n\right].
\end{aligned}
\tag{26}
$$

The kth Laplace residual function can be expressed as

$$\begin{aligned} LRes_W^k(s,p) =& W_k(s,p) - \frac{\phi_0(s)}{p} - \frac{\phi_1(s)}{p^2} - \frac{k_1}{p^2} W_{k_{ss}}(s,p) \\ & - \frac{3k_2}{p^2}\mathfrak{L}\left[\mathfrak{L}^{-1}[W_{k_s}(s,p)]^2 \mathfrak{L}^{-1}[W_{k_{ss}}(s,p)]\right] \\ & - \frac{2\alpha\varpi}{p^2}\sum_{n=0}^{\infty}\frac{(-1)^n}{n!}4^n\alpha^n\mathfrak{L}\left[\mathfrak{L}^{-1}\left[W_k(s,p)\right]^n\right] \\ & + \frac{2\alpha\varpi}{p^2}\sum_{n=0}^{\infty}\frac{(-1)^n\alpha^n}{n!}\mathfrak{L}\left[\mathfrak{L}^{-1}\left[W_k(s,p)\right]^n\right]. \end{aligned} \tag{27}$$

step 3: To obtain the coefficient functions $\phi_n(s)$, we solve the following system, iteratively:

$$\lim_{k\to\infty} p^{k+1} LRes_W^k(s,p) = 0, \qquad k = 1,2,3,\ldots. \tag{28}$$

Finally, we use the Laplace inverse on $W_k(s,p)$ to find the kth approximate solution, $w_k(s,\tau)$. Here are the first few elements of the sequence $\phi_n(s)$.

$$\begin{aligned} \phi_1(s) =& 0.332348\tanh(s), \\ \phi_2(s) =& -0.106659\ \mathrm{sech}(s)^{0.707107} + 0.113761\ \mathrm{sech}(s)^{1.41421} \\ & + \mathrm{sech}(s)^2(0.05 + 0.015\tanh(s)^2), \\ \phi_3(s) =& 0.00835513\ \mathrm{sech}(s)^{1.70711}\sinh(s) - 0.01789\ \mathrm{sech}(s)^{2.41421}\sinh(s) \\ & + 0.00332348\mathrm{sech}(s)^4\tanh(s) + \ \mathrm{sech}(s)^2(-0.0110783\tanh(s) \\ & - 0.00332348\tanh(s)^3. \end{aligned}$$

Now, the kth approximation $w_k(s,\tau)$ can be expressed as

$$\begin{aligned} w_k(s,\tau) =& -\log\left[1.09545\ \mathrm{sech}(s)\right] + 0.332348\tau\tanh(s) \\ & + \tau^2(-0.106659\mathrm{sech}(s)^{0.707107} + 0.113761\ \mathrm{sech}(s)^{1.41421} \\ & + \ \mathrm{sech}(s)^2(0.05 + 0.015\tanh(s)^2)) \\ & + \tau^3(0.00835513\ \mathrm{sech}(s)^{1.70711}\sinh(s) \\ & - 0.0178229\mathrm{sech}(s)^{2.41}\sinh(s) + 0.00332348\ \mathrm{sech}(s)^4\tanh(s) \\ & + \cdots. \end{aligned} \tag{29}$$

5 Convergence analysis

In this section, we provide a convergence analysis of the suggested method.

Theorem 3. [15] Let $W(s,p) = \mathfrak{L}[w(s,\tau)]$ be a piece-wise continuous function on $I \times [0,\infty)$. Theorem 2 can be viewed as representing the new form of Taylor's series. If $\left|s\mathfrak{L}[\partial_\tau^{n+1} w(s,\tau)]\right| \leq \mu(s)$, then finally, the following inequality is satisfied by the Laplace transform reminder $\mathfrak{R}_n$:

$$|\mathfrak{R}_n(s,p)| \leq \frac{\mu(s)}{p^{1+(n+1)}}.$$

Theorem 4. Suppose that $w_n(s,\tau)$ and $w(s,\tau)$ are defined in a Banach space over $(\mathfrak{C}[0,1], \|\cdot\|)$. The series $\{w_n(s,\tau)\}_{n=0}^{\infty}$ converges to an exact solution on the interval $0 < \mu < 1$.

Proof. Let $\mathcal{P}_n$ be the sequence of partial sum

1. $\mathcal{P}_0 = w_0(s,\tau)$,
2. $\mathcal{P}_1 = w_0(s,\tau) + w_1(s,\tau)$,
3. $\mathcal{P}_n = w_0(s,\tau) + w_1(s,\tau) + \cdots + w_n(s,\tau)$.

Now, $\mathcal{P}_n(s,\tau)_{n=0}^{\infty}$ is a Cauchy sequence. Then

$$\begin{aligned} \|\mathcal{P}_{n+1} - \mathcal{P}_n\| = \|w_{n+1}(s,\tau)\| &\leq \mu \|w_n(s,\tau))\| \leq \mu^2 \|w_{n-1}(s,\tau))\| \\ &\leq \cdots \leq \mu^{n+1} \|w_0(s,\tau)\|. \end{aligned} \tag{30}$$

Now, for every $n, m \in N$, $n \geq m$, and by using (30), we have

$$\begin{aligned} &\|\mathcal{P}_n - \mathcal{P}_m\| \\ &= \|(\mathcal{P}_n - \mathcal{P}_{n-1}) + (\mathcal{P}_{n-1} - \mathcal{P}_{n-2}) + \mathcal{P}_{n-2} + \cdots + (\mathcal{P}_{m+1} - \mathcal{P}_m)\| \\ &\leq \|(\mathcal{P}_n - \mathcal{P}_{n-1})\| + \|(\mathcal{P}_{n-1} - \mathcal{P}_{n-2})\| + \cdots + \|(\mathcal{P}_{m+1} - \mathcal{P}_m)\| \\ &\leq \mu^n \|u_0(s,\tau)\| + \mu^{n-1} \|u_0(s,\tau)\| + \cdots + \mu^{m+1} \|u_0(s,\tau)\| \\ &\leq (\mu^n + \mu^{n-1} + \cdots + \mu^{m+1}) \|u_0(s,\tau)\| \\ &= \frac{1-\mu^{n-m}}{1-\mu} \mu^{m+1} \|u_0(s,\tau)\|. \end{aligned}$$

For $0 < \mu < 1$ and $1 - \mu^{n-m} < 1$, we get

$$\|\mathcal{P}_n - \mathcal{P}_m\| \leq \frac{\mu^{m+1}}{1-\mu} \|u_0(s,\tau)\|.$$

Since $\lim_{m\to\infty}[\frac{\mu^{m+1}}{1-\mu} \|u_0(s,\tau)\|] = 0$ and $u_0(s,\tau)$ is bounded, we have

$$\lim_{n,m\to\infty} \|\mathcal{P}_n - \mathcal{P}_m\| = 0.$$

Therefore, the series converges. □

6 Numerical examples

To demonstrate the performance of numerical simulations various initial values are provided for solving the nonlinear PBD model using the methods RSPM and LRPSM. We use a PC with a Ryzen 5 (3500U) processor for the computation. The MATHEMATICA software is used to construct problems and plot two-dimensional and three-dimensional graphs for different values of s and τ.

Example 1. Consider the PBD model, (4). The exact solution for this problem is provided by

$$w(s,\tau) = \frac{-1}{\alpha} \ln\left(\pm\frac{2\sqrt{3}\sqrt{k_2}}{\alpha^2\sqrt{\Omega}} \operatorname{sech}^2(s-\beta\tau)\right).$$

Also, the initial condition is given by

$$u(s,0) = \frac{-1}{\alpha} \ln\left(\pm\frac{2\sqrt{3}\sqrt{k_2}}{\alpha^2\sqrt{\Omega}} \operatorname{sech}^2 s\right), \tag{31}$$

where $\alpha = 1, \Omega = 0.1, k_1 = 0.1, k_2 = 0.01, \beta = 0.332348, \tau = 1$.

Table 1 compares the approximate solutions derived by the RPSM and LRPSM methods for $w_5(s,\tau)$ to their exact solutions, as well as the absolute errors. Even though there are few approximation methods for solving the PBD dynamic model, the authors compare their results to the exact answer that has been verified. Table 2 compares the maximum absolute errors solved using the FD method [3] with the RPSM and LRPSM for solving the PBD model. Figures 1 and 2 display a two-dimensional graph of the approximate solutions for different values of $\tau = 1, 2, 3$. Figure 3 provides a comparison

Table 1: Comparison table for $w_5(s,\tau)$

s	τ	Exact solution	RPSM	LRPSM
0.1	0.1	-0.0823111525861	2.02289×10^{-6}	1.14496×10^{-8}
	0.2	-0.07736822772221	9.14133×10^{-6}	5.62125×10^{-8}
	0.3	-0.07135098243578	2.13121×10^{-6}	1.2389×10^{-8}
	0.4	-0.06427226132232	3.93493×10^{-6}	2.06541×10^{-8}
0.2	0.1	-0.06420461254424342	3.06466×10^{-6}	4.21426×10^{-8}
	0.2	-0.06420461254424342	1.27704×10^{-6}	4.21426×10^{-8}
	0.3	-0.04690604169269628	2.99501×10^{-6}	4.99988×10^{-8}
	0.4	-0.036731130920844575	5.55226×10^{-6}	6.74669×10^{-8}
0.3	0.1	-0.03663619985626926	4.37628×10^{-6}	7.41591×10^{-8}
	0.2	-0.025462077770375065	7.85772×10^{-6}	1.40389×10^{-8}
	0.3	-0.013319517915262057	4.25469×10^{-6}	1.40389×10^{-8}
	0.4	-0.00023174466185355724	2.02289×10^{-6}	2.35173×10^{-8}
0.4	0.1	-0.00011122438946878011	6.05776×10^{-6}	2.31873×10^{-8}
	0.2	0.01390542657263386	2.50589×10^{-6}	8.77949×10^{-8}
	0.3	0.028817222671667767	5.82749×10^{-6}	2.12122×10^{-8}
	0.4	0.04459787305092009	1.0702×10^{-6}	4.11488×10^{-8}

of RPSM and LRPSM employing the exact solution. Figures 4 and 5 show a three-dimensional graph of the approximate solution. Tables 3 and 4 display the CPU time required to solve the PBD model using the RPSM and LRPSM techniques for various values of $w_k(s,\tau)$, respectively. The obtained results have been compared with the same obtained by some existing methods. It manifests that the RPSM is more accurate than the LRPSM, and the computational time taken by both techniques is much less (less than a second)

Example 2. Consider the PBD model defined in (5). The exact solution and initial conditions for this problem are provided by

$$w(s,\tau) = \frac{-1}{\alpha} \ln\left(\frac{2\sqrt{3}\sqrt{k_2}}{\alpha^2\sqrt{\Omega}} \frac{e^{s-\beta\tau}}{(1+e^{s-\beta\tau})^2}\right),$$

Table 2: Comparison L_∞ errors for Example 1

s	RPSM	LRPSM	FD method[3]
-1	2.65558×10^{-6}	6.74669×10^{-7}	2.24109×10^{-5}
0	9.66568×10^{-7}	7.41549×10^{-8}	1.68698×10^{-4}
1	3.50922×10^{-6}	2.35565×10^{-7}	3.58976×10^{-5}

Table 3: CPU time of Example 1 for $w_5(s,\tau)$, $w_7(s,\tau)$, and $w_9(s,\tau)$ using RPSM

$w_5(s,\tau)$	$w_7(s,\tau)$	$w_9(s,\tau)$
0.246 /s	0.443/s	0.689/s

Table 4: CPU time of Example 1 for $w_5(s,\tau)$, $w_7(s,\tau)$ and $w_9(s,\tau)$ using LRPSM

$w_5(s,\tau)$	$w_7(s,\tau)$	$w_9(s,\tau)$
0.149 /s	0.248/s	0.487/s

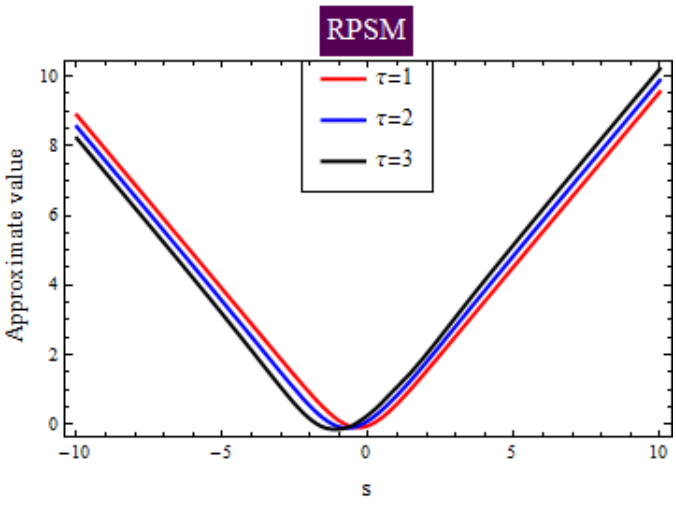

Figure 1: Approximate solution using RPSM for $\tau = 1, 2, 3$

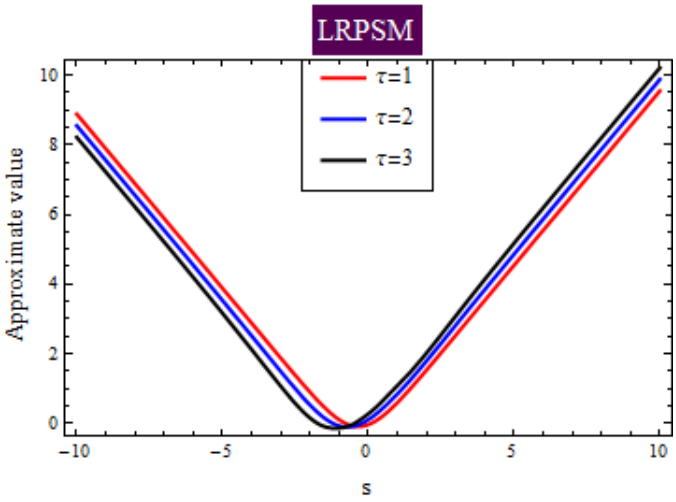

Figure 2: Approximate solution using LRPSM for $\tau = 1, 2, 3$

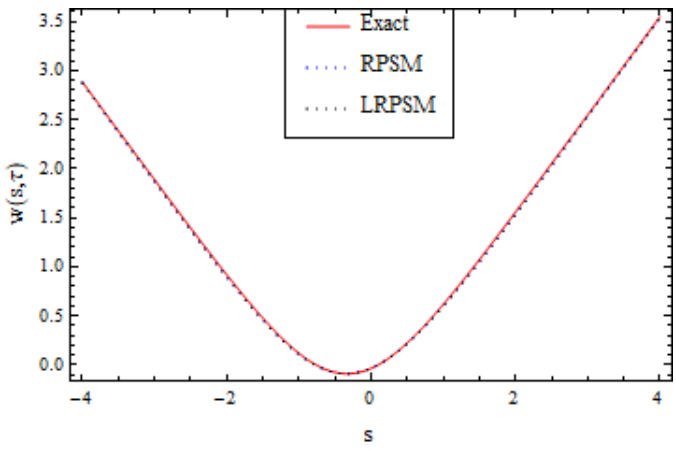

Figure 3: Comparison of RPSM and LRPSM with exact solution

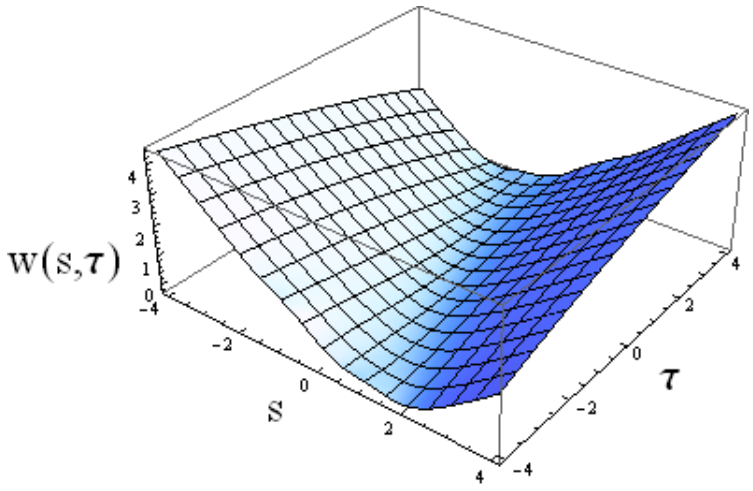

Figure 4: Approximate solution using RPSM

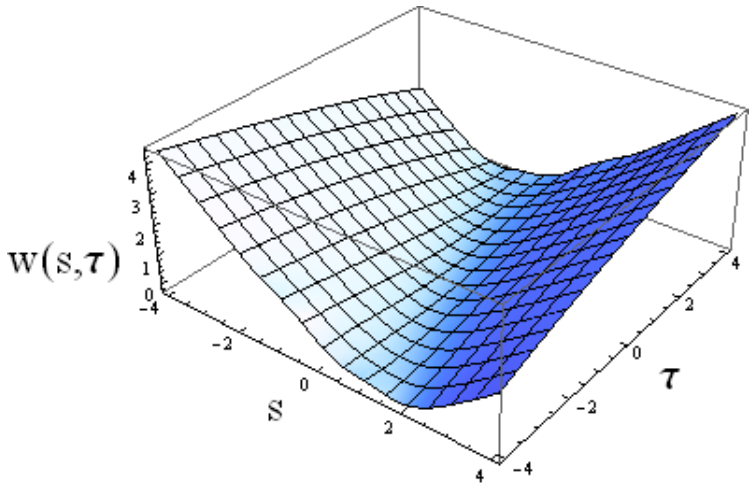

Figure 5: Approximate solution using LRPSM

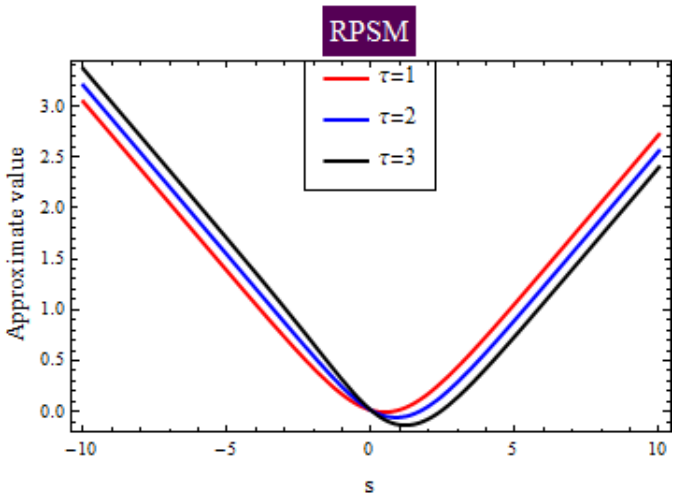

Figure 6: Approximate solution using RPSM for $\tau = 1, 2, 3$

$$w(x,0) = \frac{-1}{\alpha} \ln\left(\frac{2\sqrt{3}\sqrt{k_2}}{\alpha^2\sqrt{\Omega}} \frac{e^s}{(1+e^s)^2}\right), \tag{32}$$

where $\alpha = 3, \Omega = 0.1, k_1 = 0.1, k_2 = 0.01, \beta = 0.483656, \tau = 1$.

Table 5 displays the exact solution for the PBD model and compares absolute errors with the RPSM and LRPSM techniques with $w_5(s,\tau)$. Although there are few approximation approaches for solving the PBD model equation, the authors compare their results to the exact solution that has been validated. Table 6 compares the greatest absolute errors solved by the FD approach [3] with the nonlinear PBD model equation. Figures 6 and 7 illustrate a two-dimensional graph of approximate solutions for $\tau = 1, 2, 3$. Figure 8 illustrates the comparison of RPSM and LRPSM with the precise answer. Figures 9 and 10 show a three-dimensional graph of the approximate answer. Tables 7 and 8 display the CPU time required to solve the PBD model using the RPSM and LRPSM techniques for various values of $w_k(s,\tau)$, respectively.

Table 5: Comparison table for $w_5(s,\tau)$

s	τ	Exact solution	RPSM	LRPSM
0.1	0.1	0.013048991520552798	1.95404×10^{-6}	1.87035×10^{-8}
	0.2	0.012827730618851004	7.81952×10^{-6}	7.48505×10^{-8}
	0.3	0.012996302429450476	1.75981×10^{-6}	1.68458×10^{-8}
	0.4	0.013554509915358792	3.12868×10^{-6}	2.9949×10^{-8}
0.2	0.1	0.014741090120408296	1.94237×10^{-5}	1.85741×10^{-6}
	0.2	0.013715149604062494	7.77844×10^{-6}	7.4395×10^{-8}
	0.3	0.013078005647602956	1.75183×10^{-6}	1.67573×10^{-8}
	0.4	0.01283040190258303	3.11674×10^{-6}	2.98765×10^{-8}
0.3	0.1	0.016264113007539976	1.92221×10^{-6}	1.80394×10^{-8}
	0.2	0.018089633401329762	770323×10^{-6}	7.23719×10^{-8}
	0.3	0.014824428284429108	1.73614×10^{-6}	1.63285×10^{-6}
	0.4	0.013772248795808822	3.09105×10^{-6}	2.91017×10^{-6}
0.4	0.1	0.023078084980686298	1.89392×10^{-6}	1.80394×10^{-6}
	0.2	0.02046197927720671	7.59522×10^{-6}	7.23719×10^{-6}
	0.3	0.018226	1.71302×10^{-6}	1.63285×10^{-6}
	0.4	0.0163753558674409	3.05207×10^{-6}	2.91017×10^{-6}

Table 6: Comparison of L_∞ errors of Example 2

s	RPSM	LRPSM	FD method[3]
-1	8.65558×10^{-8}	8.65558×10^{-8}	7.66503×10^{-7}
0	7.66568×10^{-8}	7.66568×10^{-8}	3.46402×10^{-7}
1	9.50922×10^{-8}	8.56666×10^{-8}	7.66228×10^{-7}

Table 7: CPU time of Example 2 for $w_5(s,\tau)$, $w_7(s,\tau)$ and $w_9(s,\tau)$ using RPSM

$w_5(s,\tau)$	$w_7(s,\tau)$	$w_9(s,\tau)$
0.246 /s	0.399/s	0.611/s

Table 8: CPU time of Example 2 for $w_5(s,\tau)$, $w_7(s,\tau)$ and $w_9(s,\tau)$ using LRPSM

$w_5(s,\tau)$	$w_7(s,\tau)$	$w_9(s,\tau)$
0.151 /s	0.244/s	0.477/s

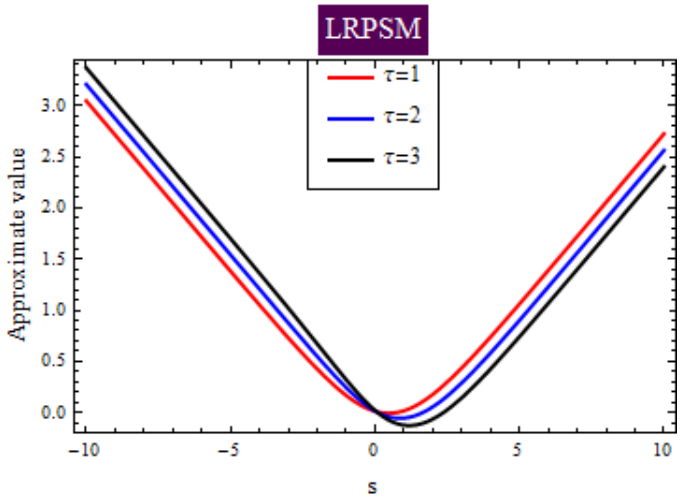

Figure 7: Approximate solution using LRPSM for $\tau = 1, 2, 3$

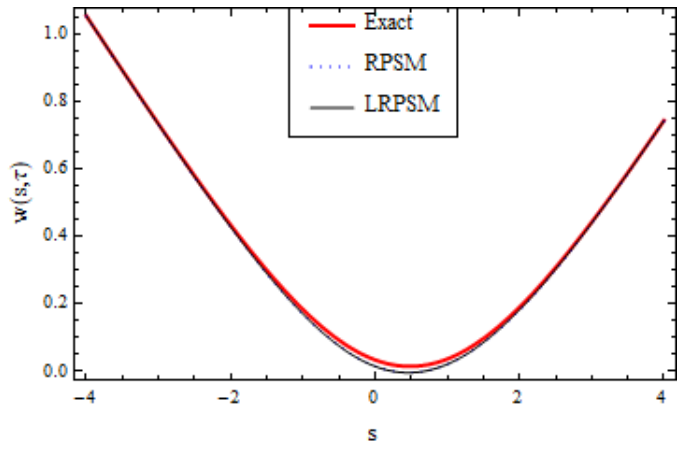

Figure 8: Comparison of RPSM and LRPSM with exact solution

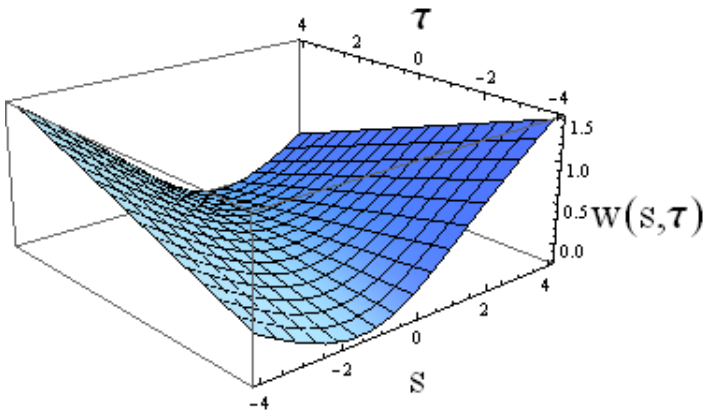

Figure 9: Approximate solution using RPSM

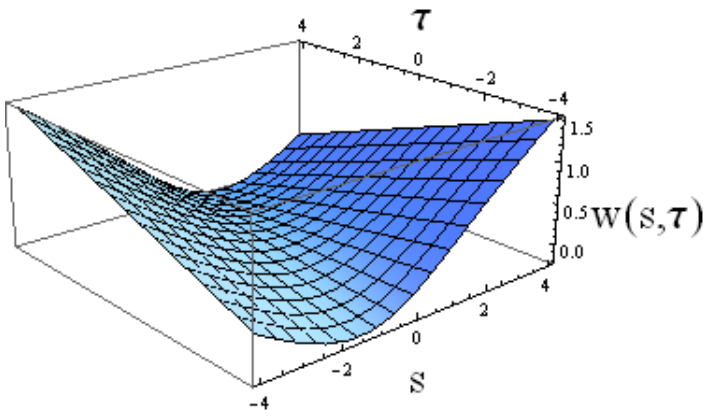

Figure 10: Approximate solution using LRPSM

7 Conclusion

The primary aim of this research was to solve the nonlinear PBD model using two semi-analytical methods: the RPSM and LRPSM. The RPSM is often simple for manual calculations and efficient when using computational tools, as it mainly involves calculating the limit at infinity, although this can be computationally expensive. In contrast, a new approach was introduced, combining the Laplace transform operator with the residual power series. The authors conducted a convergence analysis of the proposed methods. For small values of k, the method yields highly accurate results, and increasing the number of iterations improves the solution's precision. Numerical examples confirmed the reliability, accuracy, and effectiveness of the methods. A key advantage of the new technique is that it reduces the computational effort required to obtain the solution in power series form, with coefficients determined through successive algebraic steps. In conclusion, the LRPSM has demonstrated its ability to solve nonlinear equations with high accuracy and simplicity. The authors applied two methods to the Peyrard–Bishop model and compared the results, demonstrating that both methods produce very similar outcomes. However, the computational time required for the LRPSM approach is significantly less than that for the RPSM approach, as shown in tabular form.

This opens opportunities for researchers to extend the method to other types of equations, such as integral, integro-differential, and algebraic equations. Future work will involve applying this method to higher-dimensional physical problems, with a particular focus on recent developments in conformable fractional problems.

References

[1] Abazari, R., Jamshidzadeh, S. and Wang, G. *Mathematical modeling of DNA vibrational dynamics and its solitary wave solutions,* Rev. Mex. Fis. 64(6)(2018), 590–597.

[2] Agüero, M.A., De Lourdes Najera, M.A. and Carrillo, M. *Nonclassic*

solitonic structures in DNA's vibrational dynamics, Int. J. Mod. Phys. B 22(16)(2008), 2571–2582.

[3] Ali, K.K., Cattani, C., Gómez-Aguilar, J.F., Baleanu, D. and Osman, M.S. *Analytical and numerical study of the DNA dynamics arising in oscillator-chain of Peyrard-Bishop model,* Chaos Solit. Fractals. 139(2020), 110089.

[4] Al-Smadi, M., Freihat, A., Khalil, H., Momani, S. and Ali Khan, R. *Numerical multistep approach for solving fractional partial differential equations,* Int. J. Comput. Methods, 14(03) (2017), 1750029.

[5] Alvarez, A., Romero, F.R., Archilla, J.F., Cuevas, J. and Larsen, P. *Breather trapping and breather transmission in a DNA model with an interface,* Eur. Phys. J. B 51(2006), 119–130.

[6] Bayrak, M.A. and Demir, A. *A new approach for space-time fractional partial differential equations by residual power series method,* Appl. Math. Comput. 336(2018), 215–230.

[7] Behbahan, A. S., Alizadeh, A. A., Mahmoudi, M., Shamsborhan, M., Al-Musawi, T. J.and Pasha, P. *A new Adomian decomposition technique for a thermal analysis forced non-Newtonian magnetic Reiner-Rivlin viscoelastic fluid flow,* Alex. Eng. J. 80(2023), 48–57.

[8] Benhammouda, B. *The differential transform method as an effective tool to solve implicit Hessenberg index-3 differential-algebraic equations,* J. Math. 2023(1)(2023), 3620870.

[9] Chabchoub, A., Hoffmann, N.P. and Akhmediev, N. *Rogue wave observation in a water wave tank,* Phys. Rev. Lett. 106(20)(2011), 204502.

[10] Chakrabarty, A.K., Roshid, M.M., Rahaman, M.M., Abdeljawad, T. and Osman, M.S., *Dynamical analysis of optical soliton solutions for CGL equation with Kerr law nonlinearity in classical, truncated M-fractional derivative, beta fractional derivative, and conformable fractional derivative types,* Results Phys. 60, (2024) 107636.

[11] Chen, F.F. *Introduction to plasma physics and controlled fusion,* New York, Plenum press,1 (1984), 19–51.

[12] Chen, Y.Q., Tang, Y.H., Manafian, J., Rezazadeh, H. and Osman, M.S., *Dark wave, rogue wave and perturbation solutions of Ivancevic option pricing model,* Nonlinear Dyn.105 (2021) 2539–2548.

[13] Dauxois, T. *Dynamics of breather modes in a nonlinear "helicoidal" model of DNA,* Phys. Lett. A, 159(8-9) (1991), 390–395.

[14] Dusuel, S., Michaux, P. and Remoissenet, M. *From kinks to compacton-like kinks,* Phys. Rev. E, 57(2)(1998), 2320.

[15] El-Ajou, A. *Adapting the Laplace transform to create solitary solutions for the nonlinear time-fractional dispersive PDEs via a new approach,* Eur. Phys. J. Plus 136(2)(2021), 229.

[16] El-Ajou, A. and Al-Zhour, Z. *A vector series solution for a class of hyperbolic system of Caputo time-fractional partial differential equations with variable coefficients,* Front. Phys, 9(2021), 525250.

[17] El-Ajou, A., Arqub, O.A. and Momani, S. *Approximate analytical solution of the nonlinear fractional KdV–Burgers equation: a new iterative algorithm,* J. Comput.l Phys. 293(2015),81–95.

[18] Hossain, M.N., Miah, M.M., Ganie, A.H., Osman, M.S. and Ma, W.X., *Discovering new abundant optical solutions for the resonant nonlinear Schrödinger equation using an analytical technique,* Opt. Quantum Electron. 56(5), |(2024) 847.

[19] Hosseini, K., Alizadeh, F., Hinçal, E., Kaymakamzade, B., Dehingia, K. and Osman, M.S., *A generalized nonlinear Schrödinger equation with logarithmic nonlinearity and its Gaussian solitary wave,* Opt. Quantum Electron. 56(6) (2024) 929.

[20] İnç, M., Korpinar, Z. S., Al Qurashi, M. M. and Baleanu, D. *A new method for approximate solutions of some nonlinear equations: Residual power series method,* Adv. Mech. Eng. 8(4)(2016), 1687814016644580.

[21] Iqbal, M.A., Ganie, A.H., Miah, M.M. and Osman, M.S., *Extracting the ultimate new soliton solutions of some nonlinear time fractional PDEs via the conformable fractional derivative,* Fractal Fract. 8(4) (2024) 210.

[22] Kumar, S., Dhiman, S.K., Baleanu, D., Osman, M.S. and Wazwaz, A.M., *Lie symmetries, closed-form solutions, and various dynamical profiles of solitons for the variable coefficient (2+ 1)-dimensional KP equations,* Symmetry, 14(3), (2022) 97.

[23] Linak, M.C., Tourdot, R. and Dorfman, K.D. *Moving beyond Watson–Crick models of coarse grained DNA dynamics,* J. Chem. Phys. 135(20)(2011) 5102.

[24] Liu, J., Nadeem, M., Osman, M.S. and Alsayaad, Y., 2024. *Study of multi-dimensional problems arising in wave propagation using a hybrid scheme,* Sci. Rep.14(1), (2024) 5839.

[25] Osman, M.S., *Multi-soliton rational solutions for quantum Zakharov-Kuznetsov equation in quantum magnetoplasmas,* Waves in Random and Complex Media, 26(4), (2016) 434–443.

[26] Peregrine, D.H. *Water waves, nonlinear Schrödinger equations and their solutions,*ANZIAM J. 25(1) (1983),16-43.

[27] Peyrard, M. and Bishop, A.R. *Statistical mechanics of a nonlinear model for DNA denaturation,* Phys. Rev. Lett. 62(23)(1989), 2755.

[28] Priyadarsini, D., Routaray, M. and Sahu, P.K., *A new numerical approach to the solution of the nonlinear Kawahara equation by using combined Taylor–Dickson approximation,* Iranian Journal of Numerical Analysis and Optimization, 14(1), (2024) 20–43.

[29] Priyadarsini, D., Sahu, P.K. and Routaray, M., *A Combined Taylor–Bernstein Approximation for Solving Non-linear Fitz-Hugh–Nagumo Equation,* Inter. J. Appl. Comput. Math. 10(3), (2024) 110.

[30] Rahman, M.M., Murshed, M.M. and Akhter, N. *Applications of the homotopy perturbation method for some linear and non-linear partial*

differential equations, Desimal: Jurnal Matematika, 6(2) (2023), 185–190.

[31] Sarker, S., Karim, R., Akbar, M.A., Osman, M.S. and Dey, P., *Soliton solutions to a nonlinear wave equation via modern methods,* J. Umm Al-Qura Univ.Appl. Sci. (2024)1–8.

[32] Yong, Z.,Li, P. *On the time-fractional Navier–Stokes equations,* Comput. Math. Appl, 73(2017), 874–891.

[33] Zdravković, S. and Satarić, M.V. *Parameter selection in a Peyrard–Bishop–Dauxois model for DNA dynamics,* Phys. Lett. A, 373(31)(2009), 2739–2745.